

Nonradiative relaxation processes in condensed phases: Quantum versus classical baths

S. A. Egorov

Theoretical Chemistry Institute and Department of Chemistry, University of Wisconsin, Madison, Wisconsin 53706

Eran Rabani and B. J. Berne

Department of Chemistry, Columbia University, 3000 Broadway, New York, New York 10027

(Received 3 November 1998; accepted 16 December 1998)

We consider the problem of calculating the nonradiative multiphonon transition rate between two electronic states of an impurity embedded in a condensed-phase environment, where all the nuclear degrees of freedom of the bath are taken in the harmonic approximation, and the two electronic states are coupled to the bath diagonally and off-diagonally. The diagonal coupling term includes displacements of the equilibrium positions of the bath modes, the frequency shifts, and Duschinsky rotations of the bath modes between the two electronic states. We consider two forms of the off-diagonal coupling term—the first assumes that this term is independent of the nuclear degrees of freedom, and thus the coupling between the two *diabatic* electronic states is taken to be a constant; the second is based on the Born–Oppenheimer method in which the off-diagonal coupling term between the two *adiabatic* electronic states is taken to be a function of the bath momenta operators. This general model is used to examine the accuracy of several commonly used mixed quantum-classical approximations where the two electronic states are treated quantum mechanically while the bath modes are treated classically. We use the lowest-order perturbation theory to calculate the transition rate between the two electronic states, which is given in terms of the Fourier transform of the off-diagonal coupling-element time correlation function. Following the methodology of Kubo and Toyozawa, we obtain an analytic solution for the fully quantum mechanical time correlation function, and extend our method [S. A. Egorov, E. Rabani and B. J. Berne, *J. Chem. Phys.* **108**, 1407 (1998)] to obtain its mixed quantum–classical counterpart. It is shown that the nonradiative transition rate between the two electronic states calculated using the mixed quantum-classical treatment can deviate by several orders of magnitude from the exact quantum mechanical result. However, the agreement is improved when the classical time propagation of the bath modes is performed with the arithmetic average of the ground- and excited-state nuclear Hamiltonians, and thermal averaging over the initial *classical distribution* is replaced with the averaging over the corresponding *Wigner distribution*. © 1999 American Institute of Physics. [S0021-9606(99)51811-4]

I. INTRODUCTION

Nonradiative decay is a ubiquitous step in numerous chemical and physical processes, such as internal conversion, intramolecular vibrational redistribution, and intermolecular energy relaxation.^{1–4} Radiationless relaxation processes in condensed phases involve energy transfer from electronically or vibrationally excited impurities to the host. It is often the case that the amount of energy transferred exceeds by a large factor the typical energy associated with the thermal motion of the solvent. Clearly, many quanta of the bath excitations must be created in this process, which is commonly referred to as multiphonon relaxation (MPR).

A generic example of such a process is provided by the nonradiative relaxation of a localized solvated electron. Due to the strong coupling to the solvent, the transitions between the bound states of a solvated electron lead to significant solvent reorganizations. As such, this system serves as a sensitive probe of the effects of the solvent structure and dynam-

ics on the nonradiative transitions, and has received considerable experimental^{5,6} and theoretical^{7–14} attention. Most theoretical work in this field has been based on a model of a quantum solute in a classical solvent, with various levels of approximations used to account for the quantum nature of the solvent. Before discussing the ramifications of such mixed quantum–classical treatments in detail, we will briefly summarize the existing theoretical approaches to MPR in general.

Most theoretical treatments of MPR are based on the time-dependent perturbation theory. One starts by writing the total Hamiltonian as a sum of the zeroth-order Hamiltonian (whose eigenstates are typically known) and the perturbation term, which induces transitions between the zeroth-order eigenstates. Due to some arbitrariness in defining the zeroth-order Hamiltonian and the coupling term, various routes to nonradiative decay are possible. The existing theories generally involve one of the two approaches: the adiabatic (Born–

Oppenheimer) or “static-coupling” (crude Born–Oppenheimer) methods. The first method is usually invoked when discussing relaxation between electronic states, but can be applied to high-frequency vibrations as well. The coordinates are divided into fast (electronic or high-frequency vibration) and slow (bath modes) components. One neglects for the moment the kinetic energy of the bath, and finds the eigenstates of the Hamiltonian for fixed solvent coordinates. The eigenvalues of this procedure generate the usual adiabatic potential surfaces, and transitions between these surfaces are due to the “nonadiabatic” coupling (solvent kinetic energy) term in the full Hamiltonian. In solid-state theory, this approach was employed by Kubo and Toyozawa,¹⁵ Perlin,¹⁶ Miyakawa and Dexter,¹⁷ and others.^{1,18–22} Recently, this approach has become widely used in the field of liquid phase chemistry in the context of calculating nonradiative relaxation rates of solvated electrons.^{11,12,14}

The second approach can be summarized as follows: one assumes that the total Hamiltonian can be written as $H = H_{\text{TLS}} + H_b + H_1$, where H_{TLS} is the Hamiltonian for the two relevant quantum levels of the impurity (two-level system or TLS), H_b is the Hamiltonian of the bath, and H_1 is the interaction between the impurity and bath degrees of freedom. Depending on the form of H_1 , different routes to multiphonon relaxation are possible; the two most common ones involve “shifted/distorted surfaces” and “high-order coupling” schemes. In the shifted/distorted surfaces approach, the diagonal matrix elements of H_1 (in the basis that diagonalizes H_{TLS}) are functions of bath coordinates. This produces different potential energy surfaces for each state of the TLS, and in the lowest-order perturbation theory, off-diagonal matrix elements of H_1 yield multiphonon transitions. Mathematically, this route is similar to the adiabatic approach discussed above, and it has been developed quite extensively.^{1,23–32} In the high-order coupling approach, the diagonal matrix elements of H_1 are taken to be constant, while the off-diagonal matrix elements are nonlinear functions of the bath coordinates, which again allows for multiphonon processes in the lowest-order perturbation theory. This is the most common and straightforward theoretical approach to MPR, and it has been discussed by many authors.^{1,31,33–46} The relative importance of the shifted/distorted surfaces versus high-order coupling approach in calculating MPR rates has been analyzed both for vibrational^{47,48} and electronic transitions.³¹ In the case of vibrational relaxation, the high-order coupling mechanism has been shown to dominate the rate. This result is due to the fact that the change in the impurity internal vibrational state has only a small effect on its coupling to the bath, and therefore the potential energy surfaces corresponding to different states of the impurity do not differ appreciably. On the other hand, upon electronic transition, the impurity–bath coupling can be altered significantly, and the relaxation mechanism due to the distortion of potential energy surfaces may become dominant.

The methods of calculating MPR rates discussed above are quite general, and formally apply both to crystalline and liquid hosts. However, their practical realization differs sig-

nificantly in these two cases. In particular, the low-temperature solids can be treated in the harmonic approximation, which allows for the fully quantum mechanical calculation of the transition rates. At the same time, the quantum dynamics in liquid hosts is much more difficult to handle computationally, and a common approach is to employ a mixed quantum–classical treatment (quantum TLS in a classical bath). Within this framework, one is faced with the problem of inferring fully quantum mechanical rates from the results of the mixed quantum–classical simulations. The exact prescription for doing this is known only for certain simple models.⁴⁹ In the general case, the exact solution to this problem is, of course, unknown, and various approximate schemes for incorporating quantum effects have been proposed.^{11,12,14,45,46,50}

Given the approximate nature of these “correction schemes,” it is of great importance to assess their accuracy by studying exactly solvable models. One such study was recently carried out by two of us in the context of vibrational energy relaxation in condensed phases.⁴⁵ It was mentioned earlier that within the crude Born–Oppenheimer method, the high-order coupling route gives the dominant contribution to the vibrational relaxation rate. Accordingly, this particular route was considered in Ref. 45. Specifically, the bath Hamiltonian H_b was taken to be harmonic, and the coupling term H_1 was written as an exponential function of the bath coordinates. It was shown that the fully quantum relaxation rate and the rate obtained from the mixed quantum–classical treatment can differ by several orders of magnitude for sufficiently high vibrational frequencies of the impurity. In order to relate this result to the studies of vibrational relaxation in liquids, a model based on Lennard-Jones interactions was considered, and an approximate “quantum correction” for the relaxation rates was derived by mapping this model onto an effective harmonic bath. The quantum correction factor was found to depend nearly exponentially on the vibrational transition frequency of the impurity.

In view of the above findings, which illustrate the importance of solvent quantum effects for the relaxation rates involving high-frequency vibrational modes, it would be of interest to perform a similar study for the *electronic* nonradiative relaxation, where typical energy gaps exceed many times those associated with vibrational transitions; therefore, quantizing the solvent can be expected to have an even stronger effect on the relaxation rates. This issue is of particular importance in view of the recent theoretical work on the nonradiative relaxation of solvated electrons, where the quantum transition rates are often obtained from quantum–classical molecular dynamics simulations.¹² The expression for transition rates in Ref. 12 involves certain time-correlation functions, which are evaluated in terms of the trajectories of a purely classical solvent. In order to account for the quantum nature of the bath, these classical correlation functions are identified with the corresponding *symmetrized* quantum time correlation functions, thus ensuring that the transition rates obey the detailed balance condition.⁵¹ However, the study of vibrational energy relaxation based on an exactly solvable model has shown that this particular method of building in the detailed balance is the least accurate

among the available quantum correction schemes.^{45,49,52} A similar study of electronic relaxation processes would enable one to gain some insight into the relation between the quantum electronic transition rates and the semiclassical approximations to them. This is precisely the goal of the present work. Since the high-order coupling mechanism has been extensively treated in the context of vibrational relaxation,⁴⁵ we focus here on the other two routes to MPR: the “distortion dominated limit” of the static-coupling method, and the Born–Oppenheimer approach, where the electronic transitions are induced by the nonadiabatic coupling arising from the nuclear kinetic energy.

The organization of the paper is as follows. In Sec. II we introduce our model Hamiltonian and give expressions for quantum and semiclassical electronic transition rates. In Sec. III we further specify our model and calculate the transition rates within the static-coupling method. We consider separately two cases: shifted¹¹ and shifted/distorted^{28,30} multidimensional harmonic potential energy surfaces. In Sec. IV, similar calculations are performed within the Born–Oppenheimer approach. In Sec. V, we conclude.

II. MODEL HAMILTONIAN AND ELECTRONIC RELAXATION RATES

We consider an impurity embedded in a condensed phase environment, which we model as a harmonic bath. The impurity has two relevant quantum levels—initial (excited) and final (ground), which we label as $|1\rangle$ and $|0\rangle$, respectively; their energies are E_1 and E_0 . We write a general Hamiltonian for a TLS coupled (diagonally and off-diagonally) to a bath

$$H = H_0|0\rangle\langle 0| + H_1|1\rangle\langle 1| + V_{01}|0\rangle\langle 1| + V_{10}|1\rangle\langle 0|, \quad (1)$$

where $H_0 = E_0 + H'_b + \Delta_0$ and $H_1 = E_1 + H'_b + \Delta_1$; H'_b , Δ_0 and Δ_1 are operators in the Hilbert space of the bath variables. Without loss of generality we set $E_0 = 0$.

As will become clear below, it is convenient to perform the following transformation of the total Hamiltonian: we add and subtract $\Delta_1|0\rangle\langle 0|$ in Eq. (1) and use the identity $|0\rangle\langle 0| + |1\rangle\langle 1| = 1$ to obtain

$$H = (H_b + \Delta)|0\rangle\langle 0| + (\hbar\omega_{el} + H_b)|1\rangle\langle 1| + V_{01}|0\rangle\langle 1| + V_{10}|1\rangle\langle 0|, \quad (2)$$

where $\hbar\omega_{el} = E_1 - E_0$, $H_b = H'_b + \Delta_1$ and $\Delta = \Delta_0 - \Delta_1$. H_b is the bath Hamiltonian which we take to be a sum over harmonic mass-weighted normal modes Q_α with frequencies ω_α and conjugate momenta P_α

$$H_b = \frac{1}{2} \sum_{\alpha} (P_{\alpha}^2 + \omega_{\alpha}^2 Q_{\alpha}^2). \quad (3)$$

With the above form of the total Hamiltonian, it is clear that the Hamiltonian corresponding to the excited state of the TLS is given by H_b , while the Hamiltonian corresponding to the ground state is given by $H_b + \Delta$. This form of the Hamiltonian is the most convenient choice for the present problem, yet it is completely general within the harmonic model.

As discussed in the introduction, we use the lowest order perturbation theory to calculate the transition rate between the states of the TLS

$$k_{0 \leftarrow 1} = \frac{1}{\hbar^2} \int_{-\infty}^{\infty} dt e^{i\omega_{el}t} \left\langle V_{10}(t) \times \exp_{\vec{T}} \left\{ -\frac{i}{\hbar} \int_0^t dt' \Delta(t') \right\} V_{01}(0) \right\rangle. \quad (4)$$

In the above, $\langle \dots \rangle$ denotes the quantum mechanical average over the bath coordinates performed with H_b (i.e., the nuclear Hamiltonian corresponding to the initial state of the impurity); \vec{T} is the time-ordering operator, and both $\Delta(t)$ and $V_{10}(t)$ are the Heisenberg form for the diagonal and off-diagonal coupling terms Δ and V_{10} , respectively, and are given by

$$\Delta(t) = e^{iH_b t} \Delta e^{-iH_b t}, \quad (5)$$

$$V_{10}(t) = e^{iH_b t} V_{10} e^{-iH_b t}. \quad (6)$$

We have assumed that the TLS in the initial (excited) state reaches equilibrium with the bath prior to the occurrence of the relaxation process.

So far, our treatment has been fully quantum mechanical. Since the main interest of the present work concerns the consequences of the classical treatment of the solvent, we also provide an expression for the transition rate when the bath dynamics is treated classically⁵³

$$k_{0 \leftarrow 1} = \frac{1}{\hbar^2} \int_{-\infty}^{\infty} dt e^{i\omega_{el}t} \left\langle \exp \left\{ -\frac{i}{\hbar} \int_0^t dt' \Delta(t') \right\} \times V_{10}(t) V_{01}(0) \right\rangle_{cl}, \quad (7)$$

where $\langle \dots \rangle_{cl}$ denotes a classical equilibrium average over initial coordinates and momenta performed with H_b . $\Delta(t)$ and $V_{10}(t)$ are no longer Heisenberg operators, but rather functions of dynamic classical variables, whose time dependence is governed by H_b (see below), and the time ordering is no longer necessary. This semiclassical approximation has been recently discussed by us in the context of calculating vibronic absorption spectra of chromophores in condensed phase environment, where a similar model has been employed.^{54,55} This approach [which we have termed the dynamical classical limit (DCL)] is one of the most widely used semiclassical approximations. In particular, the study of nonadiabatic transitions of solvated electrons¹² mentioned in the introduction has been carried out with this method. However, this semiclassical approximation is not unique, since the quantum result for the rate [Eq. (4)] can be rewritten in various different (but *equivalent*) forms leading to different semiclassical approximations, which are *not equivalent* to each other.⁵³ All these semiclassical expressions have the form of Eq. (7), but the Hamiltonian used to propagate the nuclear degrees of freedom is different in each case.^{53,56} The DCL method represents one possible choice of the propagation scheme, where the time dependence of the classical variables is governed by the initial state nuclear Hamiltonian

(H_b in the present case). Alongside the DCL scheme, in our study of vibronic spectra we have considered another semiclassical approximation, where the dynamics of the nuclear degrees of freedom is governed by the arithmetic average of the nuclear Hamiltonians corresponding to the initial and final states of the impurity (in the present case it is $H_b + \Delta/2$).⁵⁷ Accordingly, this approximation has been termed the averaged classical limit (ACL).^{54,55} This particular choice of the propagation scheme has been motivated by the analysis of the Wigner form of the quantum mechanical expression for the relevant time-correlation function.^{54,57} It has been found that the ACL method gave consistently more accurate results than the DCL approximation (in a sense of better agreement with the exact quantum results). In the present work, we will test the accuracy of both semiclassical schemes (DCL and ACL) for calculating nonradiative electronic transition rates.

It is clear from the Eqs. (4) and (7) that the central quantities in the calculation of the transition rate are the off-diagonal (V_{10}) and the diagonal (Δ) coupling terms. As discussed in the introduction, we will consider two different forms of the off-diagonal coupling: (a) V_{10} is taken to be constant (static-coupling scheme), and (b) V_{10} is the off-diagonal matrix element of the nuclear kinetic energy operator (Born–Oppenheimer method). Regarding the diagonal coupling term, we write it as a quadratic form in the phonon coordinates

$$\Delta = \sum_{\alpha} \omega_{\alpha}^2 \delta_{\alpha} Q_{\alpha} + \frac{1}{2} \sum_{\alpha} \omega_{\alpha}^2 \delta_{\alpha}^2 + \sum_{\alpha\alpha'} g_{\alpha\alpha'} Q_{\alpha} Q_{\alpha'}. \quad (8)$$

This form of diagonal coupling arises when the two potential energy surfaces corresponding to the two states of the TLS can be described by two multidimensional harmonic surfaces with different equilibrium positions and different frequencies with the additional possibility of mode mixing between the two states. The first two terms in Δ are due to the displacements of the equilibrium positions of the normal modes, while the last term corresponds to the frequency shifts and Duschinsky rotations of the normal modes between the two electronic states.

In the next section we will further specify our model, and will perform the calculations of the electronic transition rates within the static-coupling scheme both quantum mechanically and with various semiclassical approximations.

III. STATIC-COUPLING APPROACH

Under the assumption of the constant off-diagonal coupling, the quantum mechanical expression for the transition rate given by Eq. (4) reduces to the Fourier transform (evaluated at the frequency ω_{el}) of the thermal average of the time-ordered exponential

$$k_{0 \leftarrow 1} = \frac{|V_{10}|^2}{\hbar^2} \int_{-\infty}^{\infty} dt e^{i\omega_{el}t} \left\langle \exp_T \left[-\frac{i}{\hbar} \int_0^t dt' \Delta(t') \right] \right\rangle. \quad (9)$$

As discussed in the previous section, in order to obtain a semiclassical approximation to the above result, one needs to

replace the quantum mechanical average with the classical one, neglect the time ordering, and treat $\Delta(t)$ as a function of dynamic classical variables. In addition, one needs to specify the Hamiltonian used for the propagation of the classical degrees of freedom. Here, we will limit ourselves to the two aforementioned propagation schemes, i.e., the DCL and the ACL approximations.

We note that the form of the diagonal coupling term Δ given in Eq. (8) is completely general within the harmonic model. At the same time, numerous theoretical studies considered a simplified situation, where Δ is taken to be a linear function of bath coordinates.^{11,53,56,29} We will start by looking at this simple model, and then proceed to treat a more general case of quadratic diagonal coupling.

A. Linear diagonal coupling

We consider the model of two identical mutually displaced multidimensional harmonic surfaces, where the diagonal coupling term has the form

$$\Delta = \sum_{\alpha} \omega_{\alpha}^2 \delta_{\alpha} Q_{\alpha} + \frac{1}{2} \sum_{\alpha} \omega_{\alpha}^2 \delta_{\alpha}^2. \quad (10)$$

The quantum mechanical transition rate for this model has been calculated by many authors^{1,11,15}

$$k_{0 \leftarrow 1} = \frac{|V_{01}|^2}{\hbar^2} \int_{-\infty}^{\infty} dt e^{i\omega_{el}t} \exp \left\{ \frac{1}{2\hbar} \int_0^{\infty} d\omega J(\omega) \times \omega [\coth(\beta\hbar\omega/2)(\cos(\omega t) - 1) - i \sin(\omega t)] \right\}, \quad (11)$$

where the spectral density $J(\omega)$ is given by

$$J(\omega) = \sum_{\alpha} \delta_{\alpha}^2 \delta(\omega - \omega_{\alpha}). \quad (12)$$

Note that in the limit $t \rightarrow \infty$, the second exponential in the integrand in Eq. (11) decays to a constant value (which is nonzero and real). Therefore, the time integration will lead to an appearance of a delta function for $\omega_{el} = 0$. Since we are only interested in the rates of electronic transitions for nonzero (in fact, large!) energy gaps, in performing the numerical calculations of the transition rates below, we will simply subtract the above constant from the second exponential in the integrand in Eq. (11).

The dynamical classical limit of this model has also been derived,^{11,53,58} and the result reads:

$$k_{0 \leftarrow 1} = \frac{|V_{01}|^2}{\hbar^2} \int_{-\infty}^{\infty} dt e^{i\omega_{el}t} \exp \left\{ \frac{1}{\hbar^2} \int_0^{\infty} d\omega J(\omega) \times [(\cos(\omega t) - 1)/\beta - \frac{i}{2}\hbar\omega^2 t] \right\}. \quad (13)$$

The presence of \hbar in the above result stems from the semiclassical nature of the DCL approach: the two electronic levels are treated quantum mechanically, while the nuclear de-

degrees of freedom are propagated classically. Note that within the DCL approximation, the $\sin(\omega t)$ term present in the quantum mechanical result is replaced by its short-time limit. As a consequence, in the limit $t \rightarrow \infty$, the second exponential in the integrand in Eq. (13) develops an oscillatory behavior (rather than decaying to a real constant value as in the quantum-mechanical case). This makes it impossible to obtain a converged result for the DCL transition rate within this model.

The above drawback of the DCL approach is remedied in the ACL method. By following the procedure outlined in Ref. 54, one obtains the following closed-form analytical expression for the transition rate in the ACL approximation:

$$k_{0 \leftarrow 1} = \frac{|V_{01}|^2}{\hbar^2} \int_{-\infty}^{\infty} dt e^{i\omega_{el}t} \exp \left\{ \frac{1}{\hbar^2} \int_0^{\infty} d\omega J(\omega) \times \left[(\cos(\omega t) - 1)/\beta - \frac{i}{2\hbar\omega} \sin(\omega t) \right] \right\}. \quad (14)$$

The only difference of the above result from the quantum-mechanical expression given by Eq. (11) is that the $\coth(\beta\hbar\omega/2)$ is replaced by its high-temperature limit. This difference can be traced to the fact that the thermal averaging in the ACL approximation is performed with the classical probability distribution. This suggests a modification of the ACL method, where the averaging is performed instead with the Wigner distribution based on the initial state nuclear Hamiltonian.^{59,60} We will refer to this approximation as the WACL. In the present model, the latter is given by Eq. (3), and the Wigner distribution takes a simple Gaussian form.⁶¹

$$\rho_W = \prod_{\alpha} \frac{\tanh(\beta\hbar\omega_{\alpha}/2)}{\pi\hbar} \exp \left\{ -\frac{2 \tanh(\beta\hbar\omega_{\alpha}/2)}{\hbar\omega_{\alpha}} \times \left[\frac{P_{\alpha}^2}{2} + \frac{\omega_{\alpha}^2 Q_{\alpha}^2}{2} \right] \right\}. \quad (15)$$

The above form can be readily employed within our method of calculating the transition rate. It turns out that the combination of thermal averaging with the Wigner distribution and the propagation with the average Hamiltonian produces the *exact* quantum mechanical result for the rate. It is worth emphasizing that this conclusion holds only for the case of mutually displaced identical harmonic surfaces. It no longer holds in a more general situation, when the frequency shifts and/or Duschinsky rotations of (harmonic) modes are present. Needless to say, the above conclusion also breaks down in the case of anharmonic surfaces.

We now use the results given in Eqs. (11) and (14) to perform model calculations of the electronic transition rates between the identical, linearly displaced harmonic surfaces. It is clear from the above equations that this model is completely specified by a single spectral density $J(\omega)$. In the case of electronic relaxation processes (which are characterized by large transition gaps), the dominant contribution to the relaxation rate generally comes from the coupling of the impurity to the optical phonons, whose frequencies are

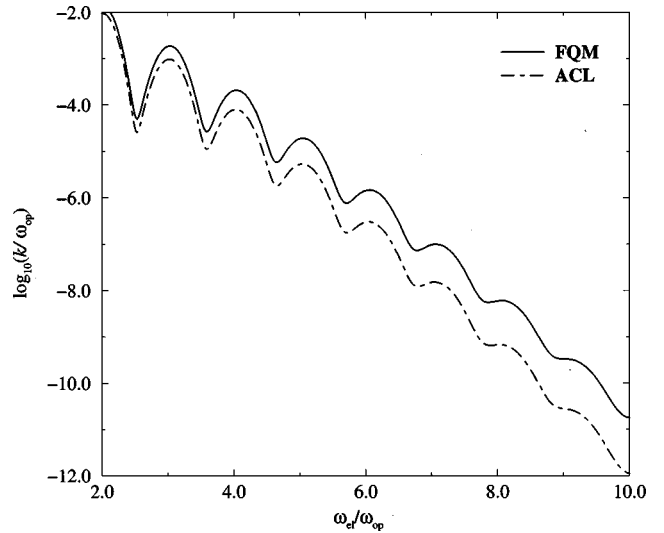


FIG. 1. Semilog plots of the nonadiabatic transition rate for linear diagonal coupling and static off-diagonal coupling as a function of the reduced electronic gap. The results for the WACL are not shown since this approximation is exact for this choice of couplings.

higher than the acoustic phonons.⁴² In order to model the corresponding spectral density, we have chosen a Gaussian form centered at ω_{op} with the width parameter σ and the normalization constant λ ²⁸

$$J(\omega) = \frac{\lambda}{(2\pi\sigma^2)^{1/2}} \exp[-(\omega - \omega_{op})^2/2\sigma^2]. \quad (16)$$

Since optical phonons are characterized by a narrow dispersion, we have limited ourselves to the case $\sigma/\omega_{op} \ll 1$, which, in addition, allows us to avoid the nonphysical contributions arising from the tail of the Gaussian function extending to negative frequencies. Specifically, we have chosen the following values of the parameters: $\omega_{op}=1.0$; $\sigma=0.1$ (from now on, we employ atomic units). With the above $J(\omega)$, we have calculated the electronic relaxation rates for the inverse temperature $\beta=4$ and the off-diagonal coupling matrix element $V_{01}=0.1$ from the fully quantum mechanical expression given by Eq. (11) and from the ACL approximation given by Eq. (14). [As discussed earlier, the transition rate in the dynamic classical limit from Eq. (13) does not converge in this case due to the nondecaying oscillatory behavior of the correlation function.]

The results of our calculations are shown in Fig. 1, where we present a semilog plot of the transition rate (scaled by ω_{op}) versus the dimensionless energy gap $\omega_{el}^* = \omega_{el}/\omega_{op}$. The frequencies of optical phonons typically lie in the range of 500–800 wave numbers, while the electronic energy gaps are generally on the order of several thousands of wave numbers. Hence, we have performed the model calculations up to the value of the reduced energy gap $\omega_{el}^*=10$. One sees that for the largest energy gap considered, the ACL approximation underestimates the transition rate by more than an order of magnitude as compared with the fully quantum mechanical (FQM) result. As stated earlier, this differ-

ence arises entirely from the fact that the thermal averaging in the ACL method is performed with the classical distribution function. When the latter is replaced by the Wigner distribution, one recovers the exact quantum mechanical result for the transition rate. Since the above conclusion rigorously holds only for the highly simplified model of the linearly displaced harmonic surfaces, it would be of interest to test the accuracy of the WACL method in a more general case; this will be done in the next subsection.

B. Quadratic diagonal coupling

Here, we consider the most general case of quadratic diagonal coupling between two multidimensional harmonic surfaces, i.e., we include both frequency shifts and mode mixing due to the Duschinsky rotations.³⁰ The fully quantum mechanical result for the transition rate is given by Eq. (9) with the operator Δ from Eq. (8). In this general case, the model cannot be solved analytically, and one has to resort to a numerical approach based on the Kubo–Toyozawa formalism. This method has been used earlier by us in the study of vibronic spectra in condensed phases,⁵⁴ and can be applied in a similar fashion to the problem at hand; the details of the implementation are listed in Ref. 54.

Since the method is limited to a finite number of bath modes N_b , we need to specify a procedure for choosing the frequencies ω_α , the linear-coupling coefficients δ_α , and the quadratic-coupling coefficients $g_{\alpha\alpha'}$. The procedure we have adopted has been motivated by our study of vibronic absorption spectra in condensed phases.^{54,55} We single out one “tagged” bath mode \tilde{Q}_1 and couple it to the remaining bath modes \tilde{Q}_α via the bilinear term $c_\alpha \tilde{Q}_1 \tilde{Q}_\alpha$ [$\alpha = 2, \dots, N_b$; the tildes on Q s serve to indicate that these modes are distinct from the ones which enter in Eq. (3)]. This is done for *both* electronic states. For simplicity, we assume that the spectral density, $\sum_\alpha c_\alpha^2 / (2\tilde{\omega}_\alpha) \delta(\omega - \tilde{\omega}_\alpha)$, which describes the coupling between the tagged mode and the remaining bath modes is again given by Eq. (16). In order to obtain the coupling coefficients c_α , we follow the procedure outlined in Ref. 54. The spectral density from Eq. (16) is discretized evenly with an increment $\delta\omega$ (thereby giving the frequencies $\tilde{\omega}_\alpha$), and the coupling coefficients are calculated according to

$$c_\alpha^2 = 2\tilde{\omega}_\alpha J(\tilde{\omega}_\alpha) \delta\omega. \quad (17)$$

The values of the peak frequency ω_{op} and the normalization constant λ are taken to be *different* in the two electronic states (ω_{op}^0 and λ_0 for the state $|0\rangle$, and ω_{op}^1 and λ_1 for the state $|1\rangle$). Similarly, the frequency of the tagged mode is taken to be different for the ground and for the excited electronic state— ω_1^0 and ω_1^1 , respectively. We now diagonalize the excited-state nuclear Hamiltonian with an appropriate unitary transformation U , thereby reducing it to the form H_b given in Eq. (3). The same transformation is subsequently applied to the ground-state nuclear Hamiltonian. Since the two Hamiltonians in their original form differ with respect to the frequency of the tagged mode and the coupling between the tagged mode and the remaining bath modes, they cannot

be diagonalized simultaneously. Consequently, the transformation of the ground-state nuclear Hamiltonian with U results in a form $H_b + \sum_{\alpha\alpha'} g_{\alpha\alpha'} Q_\alpha Q_{\alpha'}$, which allows us to obtain the quadratic coupling coefficients $g_{\alpha\alpha'}$ in Eq. (8).

In addition, we need to specify the linear coupling coefficients δ_α . We achieve this by shifting the equilibrium position of the tagged mode \tilde{Q}_1 in the original (i.e., untransformed) ground-state nuclear Hamiltonian by an amount d_0 . When the unitary transformation U is applied to the ground-state Hamiltonian (with just one mode shifted), the equilibrium positions of *all* transformed modes Q_α get displaced by δ_α , which allows us to obtain the first two terms in Eq. (8).

Admittedly, the above choice of the linear- and quadratic-coupling coefficients may seem rather restrictive. As an alternative, we have considered a somewhat different procedure, where the operator Δ is written in terms of a single collective phonon coordinate, the latter being a linear combination of the bath normal modes.⁶² While the relations between the quantum mechanical results and various semiclassical approximations for the electronic transition rates were similar in the two approaches, the first method proved to give faster convergence with respect to the number of bath modes. Therefore, in what follows, we will restrict ourselves to the procedure based on the “tagged” mode.

The semiclassical approximation to the transition rate is given by Eq. (7) (with V_{10} taken to be constant). When $\Delta(t)$ is propagated with the initial state nuclear Hamiltonian H_b , one obtains the DCL result (which does converge in the present case), while the propagation with the average Hamiltonian $H_b + \Delta/2$ corresponds to the ACL scheme. (Once again, the practical details of the calculations are exactly the same as those given in Ref. 54.) In both cases, the thermal averaging is performed with the classical probability distribution based on H_b . In an analogy to the linear-coupling case, we have also employed the WACL method.

We have calculated the electronic transition rates for the inverse temperature $\beta=4$ and the off-diagonal coupling matrix element $V_{01}=0.1$. The values for the other parameters have been taken as follows: $d_0=2.0$, $\omega_1^0=1.1$, $\omega_1^1=1.0$, $\omega_{\text{op}}^0=1.1$, $\omega_{\text{op}}^1=1.0$, $\lambda_0=0.05$, and $\lambda_1=0.125$. The results of our calculations are shown in Fig. 2, where we present a semilog plot of the transition rate (scaled by ω_{op}^1) versus the dimensionless energy gap $\omega_{\text{el}}^* = \omega_{\text{el}} / \omega_{\text{op}}^1$. One sees that for the largest energy gap considered ($\omega_{\text{el}}^*=10$), the DCL approximation underestimates the transition rate by nearly two orders of magnitude, while the ACL result is nearly one order of magnitude smaller than the quantum mechanical rate. The WACL method no longer produces the exact quantum result, but does provide a very good approximation to it (especially for the large energy gaps).

We remark that the quantum mechanical time correlation function appearing in the static-coupling approach [see Eq. (9)] is similar to the one considered in our study of vibronic absorption spectra.^{54,55} We have analyzed the Wigner form of this time-correlation function, and have arrived at the conclusion that a semiclassical treatment should employ the average Hamiltonian for the propagation of the nuclear degrees of freedom. Therefore, the good performance of the WACL method is hardly surprising. However, we emphasize that the

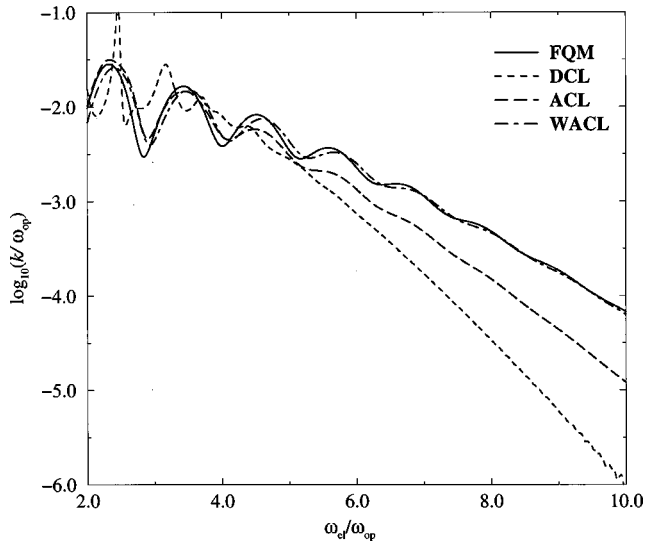


FIG. 2. Semilog plots of the nonadiabatic transition rate for quadratic diagonal coupling and static off-diagonal coupling as a function of the reduced electronic gap. Note the excellent agreement between WACL and FQM, in particular for large electronic gaps.

above conclusion is only valid for the static-coupling scheme, i.e., for the *constant* off-diagonal coupling matrix elements. It no longer holds when these matrix elements depend on the nuclear coordinates and/or momenta, as we will illustrate in the next section.

IV. BORN–OPPENHEIMER METHOD

In the Born–Oppenheimer method, the zeroth-order Hamiltonian is written as a sum of the electronic Hamiltonian (containing the electronic energy and the electron–nuclear interaction) and the nuclear potential energy operator. In contrast to the static-coupling approach, the eigenstates of the electronic Hamiltonian ($|0\rangle$ and $|1\rangle$) depend parametrically on the nuclear coordinates. The perturbation term (which induces the transitions between the two electronic states) is given by the nuclear kinetic energy operator, and its off-diagonal matrix element reads¹⁵

$$V_{10} = \sum_{\alpha} \langle 1|P_{\alpha}|0\rangle P_{\alpha} + \frac{1}{2} \sum_{\alpha} \langle 1|P_{\alpha}^2|0\rangle \equiv \vec{S} \cdot \vec{P} + \frac{1}{2} \langle 1|\vec{P}^2|0\rangle, \quad (18)$$

where we have defined two vectors \vec{P} and \vec{S} with components P_{α} and $S_{\alpha} = \langle 1|P_{\alpha}|0\rangle$, respectively. Following Kubo and Toyozawa,¹⁵ we neglect the second term in the above equation and assume S_{α} to be independent of the nuclear coordinates.

The quantum mechanical result for the electronic transition rate in the Born–Oppenheimer method is thus given by Eq. (4) with $V_{10} = \vec{S} \cdot \vec{P}$. The corresponding semiclassical approximations are obtained in exactly the same way as in the static-coupling approach. Once again, we will consider separately two cases: linear and quadratic diagonal coupling.

A. Linear diagonal coupling

The closed-form result for the quantum mechanical transition rate within this model has been given by Kubo and Toyozawa¹⁵

$$k_{0 \leftarrow 1} = \frac{|V_{10}|^2}{\hbar^2} \int_{-\infty}^{\infty} dt e^{i\omega_e t} \exp \left\{ \frac{1}{2\hbar} \int_0^{\infty} d\omega J(\omega) \times \omega [\coth(\beta\hbar\omega/2)(\cos(\omega t) - 1) - i \sin(\omega t)] \right\} \times \left\{ \left[\frac{1}{2\hbar} \int_0^{\infty} d\omega J_{\delta S}(\omega) \omega [\coth(\beta\hbar\omega/2)(\cos(\omega t) - 1) - i \sin(\omega t)] \right]^2 + \frac{1}{2\hbar} \int_0^{\infty} d\omega J_S(\omega) \omega [\coth(\beta\hbar\omega/2) \times \cos(\omega t) - i \sin(\omega t)] \right\}, \quad (19)$$

where in addition to the spectral density $J(\omega)$, we have defined two other spectral densities— $J_S(\omega)$ and $J_{\delta S}(\omega)$ as follows:

$$J_S(\omega) = \sum_{\alpha} S_{\alpha}^2 \delta(\omega - \omega_{\alpha}), \quad (20)$$

and

$$J_{\delta S}(\omega) = \sum_{\alpha} \delta_{\alpha} S_{\alpha} \delta(\omega - \omega_{\alpha}). \quad (21)$$

As in the static-coupling scheme, in the limit $t \rightarrow \infty$ the time correlation function in the integrand of Eq. (19) decays to a nonzero real constant, which we will subtract when performing the Fourier transform to calculate the transition rate.

The DCL approximation for the transition rate within this model can also be obtained in a closed form, and the result reads

$$k_{0 \leftarrow 1} = \frac{|V_{01}|^2}{\hbar^2} \int_{-\infty}^{\infty} dt e^{i\omega_e t} \exp \left\{ \frac{1}{\hbar} \int_0^{\infty} d\omega J(\omega) \times [(\cos(\omega t) - 1)/\beta - \frac{i}{2}\hbar\omega^2 t] \right\} \times \left\{ \left(\frac{1}{\beta\hbar^2} \int_0^{\infty} d\omega J_{\delta S}(\omega) (\cos(\omega t) - 1) \right)^2 + \frac{1}{\beta\hbar^2} \int_0^{\infty} d\omega J_S(\omega) \cos(\omega t) \right\}. \quad (22)$$

In the long-time limit, the time-correlation function in the integrand of Eq. (22) develops an oscillatory behavior, which precludes us from obtaining a converged result for the transition rate.

Turning to the ACL approximation, we have employed the procedure outlined in Ref. 54 to obtain the following expression for the transition rate:

$$\begin{aligned}
 k_{0 \leftarrow 1} = & \frac{|V_{10}|^2}{\hbar^2} \int_{-\infty}^{\infty} dt e^{i\omega_{el}t} \exp \left\{ \frac{1}{\hbar^2} \int_0^{\infty} d\omega J(\omega) \left[(\cos(\omega t) - 1) / \beta - \frac{i}{2} \hbar \omega \sin(\omega t) \right] \right\} \\
 & \times \left\{ \left(\frac{1}{\beta \hbar^2} \int_0^{\infty} d\omega J_{\delta S}(\omega) (\cos(\omega t) - 1) \right)^2 + \frac{1}{\beta \hbar^2} \int_0^{\infty} d\omega J_S(\omega) \cos(\omega t) + \frac{i}{\beta \hbar^2} \int_0^{\infty} d\omega J_{\delta S}(\omega) \omega \sin(\omega t) \right. \\
 & \left. \times \int_0^{\infty} d\omega J_{\delta S}(\omega) (1 - \cos(\omega t)) \right\}. \tag{23}
 \end{aligned}$$

Finally, the WACL method yields:

$$\begin{aligned}
 k_{0 \leftarrow 1} = & \frac{|V_{10}|^2}{\hbar^2} \int_{-\infty}^{\infty} dt e^{i\omega_{el}t} \exp \left\{ \frac{1}{2\hbar} \int_0^{\infty} d\omega J(\omega) \omega \left[\coth(\beta \hbar \omega / 2) (\cos(\omega t) - 1) - i \sin(\omega t) \right] \right\} \\
 & \times \left\{ \left(\frac{1}{2\hbar} \int_0^{\infty} d\omega J_{\delta S}(\omega) \omega \coth(\beta \hbar \omega / 2) (\cos(\omega t) - 1) \right)^2 + \frac{i}{2\hbar} \left(\int_0^{\infty} d\omega J_{\delta S}(\omega) \omega \sin(\omega t) \right) \right. \\
 & \left. \times \left(\int_0^{\infty} d\omega J_{\delta S}(\omega) \omega \coth(\beta \hbar \omega / 2) (1 - \cos(\omega t)) \right) + \frac{1}{2\hbar} \int_0^{\infty} d\omega J_S(\omega) \omega \coth(\beta \hbar \omega / 2) \cos(\omega t) \right\}. \tag{24}
 \end{aligned}$$

Even though the diagonal-coupling term is linear in the nuclear coordinates, the above result does not coincide with the quantum mechanical one because of the dependence of the off-diagonal coupling matrix element on the nuclear momenta.

We now use the results given in Eqs. (19), (23), and (24) to perform model calculations of the electronic transition rates between the identical, linearly displaced harmonic surfaces coupled by the nuclear kinetic energy operator. In addition to $J(\omega)$, we need to specify functional forms for the two other spectral densities— $J_S(\omega)$ and $J_{\delta S}(\omega)$. For simplicity, we take $J(\omega) = J_S(\omega) = J_{\delta S}(\omega)$, with $J(\omega)$ given by Eq. (16). Setting $\omega_{op} = 1.0$; $\sigma = 0.1$, we have calculated the electronic relaxation rates for the inverse temperature $\beta = 4$ from the fully quantum mechanical expression given by Eq. (19) and from the two levels of the ACL approximation given by Eqs. (23) and (24). The results of our calculations are shown in Fig. 3, where we present a semilog plot of the transition rate (scaled by ω_{op}) versus the dimensionless energy gap $\omega_{el}^* = \omega_{el} / \omega_{op}$. One sees that for the largest energy gap considered ($\omega_{el}^* = 10$), the ACL approximation from Eq. (23) with the classical thermal averaging underestimates the transition rate by nearly an order of magnitude, while the one from Eq. (24) overestimates the rate by about the same factor. In other words, the combination of the ACL propagation scheme and the Wigner distribution-based averaging is no longer sufficient to obtain satisfactory results.

B. Quadratic diagonal coupling

Substituting $V_{10} = \vec{S} \cdot \vec{P}$ and Δ [given by Eq. (8)] into Eq. (4), one can easily carry out the quantum mechanical trace in

the coordinate representation.¹⁵ The resulting expression for the transition rate is given in Ref. 15; it is more cumbersome than in the case of linear diagonal coupling, and will not be reproduced here. The DCL approximation for the rate (which in the present case converges) and the two variants of the ACL result are equally straightforward to obtain by using the methodology similar to the one introduced by us in the study of vibronic absorption spectra.⁵⁴

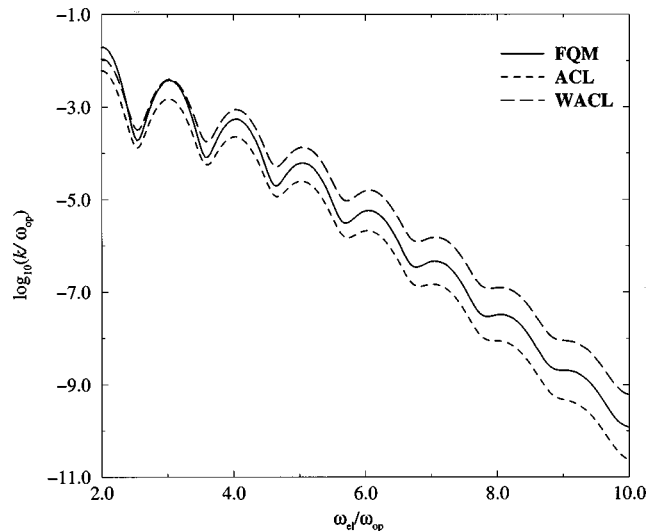


FIG. 3. Semilog plots of the nonadiabatic transition rate for linear diagonal coupling and momenta-dependent off-diagonal coupling as a function of the reduced electronic gap. Note that unlike the static off-diagonal coupling case, the WACL is no longer exact, and in fact deviates for the FQM result by almost an order of magnitude for the largest electronic gap considered.

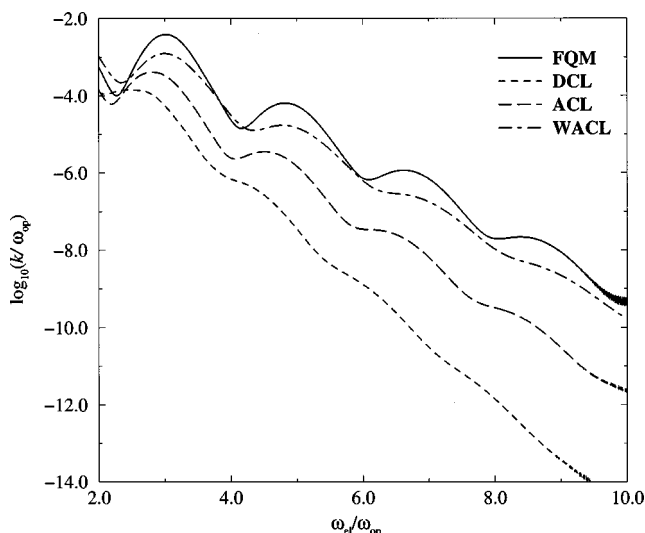


FIG. 4. Semilog plots of the nonadiabatic transition rate for quadratic diagonal coupling and momenta-dependent off-diagonal coupling as a function of the reduced electronic gap. Both DCL and ACL deviate from the FQM result by several orders of magnitude. The WACL is in much better agreement with the FQM result; however, it is not exact. The noise at large electronic gaps is due to numerical difficulties in performing the Fourier transform to obtain the rate.

In practice, the calculations of both quantum mechanical and semiclassical rates are limited to a finite number N_b of bath modes. We select the frequencies ω_α , the linear coupling coefficients δ_α , and the quadratic coupling coefficients $g_{\alpha\alpha'}$ in exactly the same way as was described in the previous section. In addition, we need to specify the components of the vector \vec{S} . As in the case of linear coupling coefficients δ_α , we start by ascribing a particular value s_0 to the tagged mode in the untransformed ground-state nuclear Hamiltonian. Upon transforming the latter with the unitary transformation which diagonalizes the excited-state Hamiltonian, one obtains the coefficients s_α for each of the bath modes.

The semiclassical approximation to the transition rate is given by Eq. (7). When $\Delta(t)$ and $V_{10}(t)$ are propagated with the initial state nuclear Hamiltonian H_b , one obtains the DCL result, while the propagation with the average Hamiltonian $H_b + \Delta/2$ corresponds to the ACL approximation (with two options for performing the thermal averaging).

We have calculated the electronic transition rates for the inverse temperature $\beta=4$. The values for the other parameters have been taken as follows: $d_0=2.0$, $s_0=2.0$, $\omega_1^0=1.1$, $\omega_1^1=1.0$, $\omega_{op}^0=1.1$, $\omega_{op}^1=1.0$, $\lambda_0=0.05$, and $\lambda_1=0.125$. The results of our calculations are shown in Fig. 4, where we present a semilog plot of the transition rate (scaled by ω_{op}) versus the dimensionless energy gap $\omega_{el}^* = \omega_{el}/\omega_{op}$. For the largest energy gap considered ($\omega_{el}^*=10$), the DCL approximation underestimates the transition rate by several orders of magnitude, while the ACL result is about two orders of magnitude smaller than the quantum mechanical rate. The WACL method still provides the best approximation to the exact quantum result, although in the present case it is less accurate compared to the static-coupling scheme.

We remark that the latter finding has certain ramifica-

tions for the semiclassical calculations of vibronic absorption spectra considered in our earlier work.^{54,55} In that work, the spectra were calculated within the Franck–Condon approximation, and the ACL method was generally found to give highly accurate results. However, if one goes beyond the Franck–Condon approximation, the off-diagonal matrix elements of the dipole operator acquire a dependence on the bath coordinates, and the analysis of the Wigner form of the corresponding time-correlation function would no longer suggest classical propagation with the average Hamiltonian. In other words, the ACL method can then no longer be expected to provide accurate results.

V. CONCLUSIONS

In this work, we have considered the problem of calculating the radiationless transition rates between the electronic states of a TLS coupled diagonally and off-diagonally to a condensed phase environment, with all the nuclear degrees of freedom treated in the harmonic approximation. Two particular routes to the nonradiative relaxation were studied: static-coupling scheme (where the coupling between the two *diabatic* electronic states was taken to be a constant), and the Born–Oppenheimer method (where the off-diagonal coupling term between the two *adiabatic* electronic states was taken to be a function of the bath momenta operators). Within each method, the diagonal coupling term was written as a general quadratic form in the bath coordinates, thereby including the displacements of the equilibrium positions of the bath modes, the frequency shifts, and Duschinsky rotations of the bath modes between the two electronic states.

The major goal of the present work has been to examine the accuracy of several commonly used mixed quantum–classical approximations in calculating the nonradiative transition rates, where the two electronic states are treated quantum mechanically while the bath modes are treated classically. We employed the lowest-order perturbation theory in the form of Fermi’s Golden Rule to calculate the transition rate between the two electronic states. The rate was written in terms of the Fourier transform of the time-correlation function for the off-diagonal coupling matrix element. Following the methodology of Kubo and Toyozawa, we have obtained an analytic result for the fully quantum mechanical time correlation function, and have extended our method^{54,55} to calculate its mixed quantum–classical counterpart. We have assumed that the nonradiative relaxation process is dominated by the coupling of the electronic degree of freedom to the optical phonons. Having introduced a model spectral density for the latter, we have calculated the transition rates both quantum mechanically and semiclassically. Our model calculations have shown that the mixed quantum–classical treatment can underestimate the transition rate by several orders of magnitude when the electronic gap is larger than the optical bath frequency. The agreement with the quantum result was improved when the classical time propagation of the bath modes was performed with the arithmetic average of the ground- and excited-state nuclear Hamiltonians and thermal averaging over the initial classical distribution was replaced with the averaging over the corresponding Wigner distribution. Nevertheless, even the latter

approach provided satisfactory results for the relaxation rates *only* within the static-coupling scheme, and was found to deviate from the quantum result appreciably in the Born–Oppenheimer method. Moreover, our study was limited to quadratic potential energy surfaces, and it is likely that for anharmonic systems the average propagation scheme with a Wigner initial distribution would fail.

It is worth noting the difference between the “mixed state propagation” method discussed above and the mean field approach (also known as the time-dependent self-consistent field).⁶³ In the latter method, the potential energy surfaces corresponding to different states of the quantum subsystem are combined to form a “mean surface” with the weights determined by the populations of the corresponding quantum states. On the other hand, in the approach discussed herein, the prescription for constructing a “mixed propagation scheme” follows from the analysis of the Wigner form of the exact quantum time kernel and its subsequent expansion in powers of the Planck’s constant. As already mentioned, the conclusion that the optimal results (for the set of systems studied here) are obtained by propagating classical degrees of freedom on the average of the ground- and excited-state potential energy surfaces, holds rigorously only for the static-coupling scheme, and is not accurate in the Born–Oppenheimer method.

Regarding the sampling of the initial conditions from the Wigner distribution function, we note that it can be performed in a straightforward fashion only for harmonic models. For more realistic anharmonic systems this distribution can become negative, and thus cannot be sampled in a simulation using a conventional method. One therefore needs to resort to approximations such as local harmonic treatment of potential energy surfaces, or perform an expansion of the Wigner distribution function in powers of the Planck’s constant (the latter approach can be expected to work only for sufficiently high temperatures). Obviously these approximations have limited range of validity and their accuracy remains to be tested.

Finally, we remark that the present study has been based entirely on the Fermi Golden Rule. One possible way to go beyond the lowest-order perturbation theory is provided by the surface-hopping technique.⁶⁴ However, similarly to the semiclassical treatments considered in this work, the surface hopping method also relies on the mixed quantum–classical (MQC) description of the system. When the coupling between the quantum states involved is weak, the perturbation theory is valid, and therefore the results from the surface-hopping calculations are expected to be similar to those obtained from the MQC perturbative approach taken in this work. The methods for improving these results (i.e., mixed state propagation and thermal averaging with the Wigner distribution) can be readily incorporated into a surface-hopping method, although the same limitations as discussed in the previous paragraphs would also apply. We also note that surface hopping breaks down for strongly avoided crossing in an anharmonic isolated system, and for this any of the above improvements are likely to fail.⁶⁵

ACKNOWLEDGMENTS

E.R. is a Rothschild and Fulbright postdoctoral fellow. This work was supported by a grant to B.J.B. from the National Science Foundation.

- ¹R. Englman, *Non-radiative Decay of Ions and Molecules in Solids* (North-Holland, Amsterdam, 1979).
- ²F. K. Fong, Editor, *Radiationless Processes in Molecules and Condensed Phases* (Springer, Berlin, 1976).
- ³S. H. Lin, Editor, *Radiationless Transitions* (Academic, New York, 1980).
- ⁴J. Jortner and R. D. Levine, *Adv. Chem. Phys.* **47**, 1 (1981).
- ⁵C. Silva, p. K. Walhout, K. Yokoyama, and P. F. Barbara, *Phys. Rev. Lett.* **80**, 1086 (1998).
- ⁶K. Yokoyama, C. Silva, D. H. Son, P. K. Walhout, and P. F. Barbara, *J. Phys. Chem. A* **102**, 6957 (1998).
- ⁷U. Landman, D. Scharf, and J. Jortner, *Phys. Rev. Lett.* **54**, 1860 (1985).
- ⁸A. Wallqvist, D. Thirumalai, and B. J. Berne, *J. Chem. Phys.* **85**, 1583 (1986).
- ⁹D. F. Coker and B. J. Berne, *J. Chem. Phys.* **89**, 2128 (1988).
- ¹⁰J. Schmitker and P. J. Rossky, *J. Chem. Phys.* **86**, 3462 (1987).
- ¹¹E. Neria and A. Nitzan, *J. Chem. Phys.* **99**, 1109 (1993).
- ¹²A. Staib and D. Borgis, *J. Chem. Phys.* **103**, 2642 (1995).
- ¹³O. V. Prezhdo and P. J. Rossky, *J. Phys. Chem.* **100**, 17094 (1996).
- ¹⁴O. V. Prezhdo and P. J. Rossky, *J. Chem. Phys.* **107**, 5863 (1997).
- ¹⁵R. Kubo and Y. Toyozawa, *Prog. Theor. Phys.* **13**, 160 (1955).
- ¹⁶Y. E. Perlin, *Sov. Phys. Usp.* **6**, 542 (1964).
- ¹⁷T. Miyakawa and D. L. Dexter, *Phys. Rev. B* **1**, 2961 (1970).
- ¹⁸F. K. Fong, S. L. Naberhuis, and M. M. Miller, *J. Chem. Phys.* **56**, 4020 (1972).
- ¹⁹S. H. Lin, *J. Chem. Phys.* **65**, 1053 (1976).
- ²⁰S. H. Lin, in *Radiationless Transitions*, edited by S. H. Lin (Academic, New York, 1980).
- ²¹B.-Z. Zhang, Y.-X. Li, M.-R. Lin, and W.-J. Chen, *Chin. Phys.* **10**, 876 (1990).
- ²²F. K. Fong, *Theory of Molecular Relaxation* (Wiley, New York, 1975).
- ²³M. D. Sturge, *Phys. Rev. B* **8**, 6 (1973).
- ²⁴D. J. Diestler, *J. Chem. Phys.* **60**, 2692 (1974).
- ²⁵D. J. Diestler, in *Radiationless Processes in Molecules and Condensed Phases*, edited by F. K. Fong (Springer, Berlin, 1976).
- ²⁶D. J. Diestler, in *Potential Energy Surfaces*, edited by K. P. Lawley (Wiley, New York, 1980).
- ²⁷R. Pässler, *Czech. J. Phys., Sect. B* **24**, 322 (1974).
- ²⁸Y. Weissman, A. Nitzan, and J. Jortner, *Chem. Phys.* **26**, 413 (1977).
- ²⁹J. Tang, *Chem. Phys.* **188**, 143 (1994).
- ³⁰J. Tang, *Chem. Phys. Lett.* **227**, 170 (1994).
- ³¹K. K. Pukhov and V. P. Sakun, *Phys. Status Solidi B* **95**, 391 (1979).
- ³²R. H. Bartram, *J. Phys. Chem. Solids* **51**, 641 (1990).
- ³³A. Nitzan, S. Mukamel, and J. Jortner, *J. Chem. Phys.* **60**, 3929 (1974).
- ³⁴A. Nitzan and R. Silbey, *J. Chem. Phys.* **60**, 4070 (1974).
- ³⁵A. Nitzan, S. Mukamel, and J. Jortner, *J. Chem. Phys.* **63**, 200 (1975).
- ³⁶J. Jortner, *Mol. Phys.* **32**, 379 (1976).
- ³⁷S. H. Lin, *J. Chem. Phys.* **61**, 3810 (1974).
- ³⁸S. H. Lin, H. P. Lin, and D. Knittel, *J. Chem. Phys.* **64**, 441 (1976).
- ³⁹Y. E. Perlin, A. A. Kaminskii, M. G. Blazha, V. N. Enakii, and V. V. Ryabchenkov, *Sov. Phys. Solid State* **24**, 386 (1982).
- ⁴⁰B. N. J. Persson, *J. Phys. C* **17**, 4741 (1984).
- ⁴¹W. E. Hagston and J. E. Lowther, *Physica (Amsterdam)* **70**, 40 (1973).
- ⁴²S. A. Egorov and J. L. Skinner, *J. Chem. Phys.* **103**, 1533 (1995).
- ⁴³S. A. Egorov and J. L. Skinner, *J. Chem. Phys.* **105**, 10153 (1996).
- ⁴⁴S. A. Egorov and J. L. Skinner, *J. Chem. Phys.* **106**, 1034 (1997).
- ⁴⁵S. A. Egorov and B. J. Berne, *J. Chem. Phys.* **107**, 6050 (1997).
- ⁴⁶D. Rostkier-Edelstein, P. Graf, and A. Nitzan, *J. Chem. Phys.* **107**, 10470 (1997).
- ⁴⁷V. P. Sakun, *Sov. Phys. Solid State* **18**, 1470 (1976).
- ⁴⁸M. Berkowitz and R. B. Gerber, *Chem. Phys.* **37**, 369 (1979).
- ⁴⁹J. S. Bader and B. J. Berne, *J. Chem. Phys.* **100**, 8359 (1994).
- ⁵⁰L. Frommhold, “Collision-induced absorption in gases,” in *Cambridge Monographs on Atomic, Molecular, and Chemical Physics*, Vol. 2 (Cambridge University Press, England, 1993).
- ⁵¹B. J. Berne and G. D. Harp, *Adv. Chem. Phys.* **17**, 63 (1970).
- ⁵²S. A. Egorov and J. L. Skinner, *Chem. Phys. Lett.* **293**, 469 (1998).
- ⁵³S. Mukamel, *J. Chem. Phys.* **77**, 173 (1982).

- ⁵⁴S. A. Egorov, E. Rabani, and B. J. Berne, *J. Chem. Phys.* **108**, 1407 (1998).
- ⁵⁵E. Rabani, S. A. Egorov, and B. J. Berne, *J. Chem. Phys.* **109**, 6376 (1998).
- ⁵⁶E. Neria and A. Nitzan, *Chem. Phys.* **183**, 351 (1994).
- ⁵⁷N. E. Shemetulskis and R. F. Loring, *J. Chem. Phys.* **97**, 1217 (1992).
- ⁵⁸A. Heidenreich and J. Jortner, *J. Chem. Phys.* **105**, 8523 (1996).
- ⁵⁹E. J. Heller, *J. Chem. Phys.* **65**, 1289 (1976).
- ⁶⁰X. Sun, H. Wang, and W. H. Miller, *J. Chem. Phys.* **109**, 7064 (1998).
- ⁶¹M. Hillery, R. F. O'Connell, M. O. Scully, and E. P. Wigner, *Phys. Rep.* **106**, 121 (1984).
- ⁶²J. L. Skinner and D. Hsu, *J. Phys. Chem.* **90**, 4931 (1986).
- ⁶³R. B. Gerber and M. A. Ratner, *Adv. Chem. Phys.* **74**, 97 (1988).
- ⁶⁴J. C. Tully, *J. Chem. Phys.* **93**, 1061 (1990).
- ⁶⁵Y. Zeiri, G. Katz, R. Kosloff, M. S. Topaler, D. G. Truhlar, and J. C. Polanyi, *Chem. Phys. Lett.* (in press).